Inorg. Chem. **2008**, *47*, 10317−10324

Metal-Dependent Assembly of a Helical-[Co_3L_3] Cluster versus a Meso-[Cu_2L_2] Cluster with O,N,N′,O′-Schiff Base Ligand: Structures and Magnetic Properties

Yuanyuan Pang, Shuxin Cui, Bo Li, Jingping Zhang,* Yu Wang, and Hong Zhang

Faculty of Chemistry, Northeast Normal University, Changchun 130024, China

Received May 11, 2008

Self-assembly of a tetradentate ligand, *N,N′*-bi(salicylidene)-2,6-pyridinediamine (H_2L), with Cu(II) or Co(II), affords a dinuclear [Cu_2L_2] complex (**1**) or a trinuclear [Co_3L_3] complex (**2**), which were characterized by the single crystal X-ray diffraction study. The coordination geometry of the Cu^{II} centers in **1** is between square planar and tetrahedral, with the ligand adopting a cis−cis conformation to give a centrally symmetric structure, which can be regarded as a mesocate. However, the coordination geometry of Co^{II} centers in **2** is distortedly tetrahedral, and the ligand adopts a cis−trans conformation. The whole complex of **2** is of a pseudo-C_3 symmatrical, torus-like structure, which can be regarded as a circular helicate. Both the mesocate and the helicate exhibit expanded supramolecular structures due to elaborate intercomplex π-stacking interactions. These two complexes were also characterized by element analysis, IR spectra, and TGA. To verify the stability of **2**, ESI-MS was carried out on both the crystal and the powdered samples. Variable temperature magnetic susceptibility measurements reveal that both **1** and **2** display antiferromagnetic properties. DFT calculations were carried out on **1** to verify the antiferromagnetic coupling between intracluster metal centers.

Introduction

Control over the arrangement and shape of coordination complexes has been a topic of considerable interest in inorganic chemistry for decades, especially since the emergence of supramolecular chemistry in the late 1970s. It provides a key to future development of designed functional materials.[1] Through careful choice of suitable ligands and metal ions, a wide variety of resultant structural motifs have been obtained, such as grids, boxes, cylinders, and helicates.[2−5] The helicate architecture has been extensively investigated in the past two decades because of its importance in the self-assembling properties and supramolecular chemistry.[6] To obtain a helical complex, it is essential to design suitable organic ligands. The ligands should contain multiple coordinating sites to match the geometrical requirement of metal centers. Furthermore, it must offer sufficient flexibility to wrap around two (or more) metal centers as a connecting strand to form a helical mode, as well as sufficient rigidity

* To whom correspondence should be addressed. E-mail: zhangjingping66@yahoo.com.cn. Tel: +86 431 85099372. Fax: +86 431 85684937.

(1) (a) Lehn, J.-M. *Pure Appl. Chem.* **1978**, *50*, 871–892. (b) Leininger, S.; Olenyuk, B.; Stang, P. J. *Chem. Rev.* **2000**, *100*, 853–908. (c) Fujita, M.; Umemoto, K.; Yoshizawa, M.; Fujita, N.; Kusukawa, T.; Biradha, K. *Chem. Commun.* **2001**, 509–518.

(2) (a) Zaworotko, M. J. *Angew. Chem., Int. Ed.* **2000**, *39*, 3052–3054. (b) Yashi, O. M.; O'Keeffe, M.; Ockwig, N. W.; Chae, H. K.; Eddaoudi, M.; Kim, J. *Nature* **2003**, *423*, 705–714.

(3) Yoshizawa, M.; Takeyama, Y.; Kusukawa, T.; Fujita, M. *Angew. Chem., Int. Ed.* **2002**, *41*, 1347–1349.

(4) Johnson, D. W.; Xu, J. D.; Saalfrank, R. W.; Raymond, K. N. *Angew. Chem., Int. Ed.* **1999**, *38*, 2882–2885.

(5) (a) Albrecht, M.; Dehn, S.; Fröhlich, R. *Angew. Chem., Int. Ed.* **2006**, *45*, 2792–2794. (b) Bermejo, M. R.; González-Noya, A. M.; Pedrido, R. M.; Romero, M. J.; Vázquez, M. *Angew. Chem., Int. Ed.* **2005**, *44*, 4182–4187. (c) Habermehl, N. C.; Angus, P. M.; Kilah, N. L.; Noren, L.; Rae, A. D.; Willis, A. C.; Wild, S. B. *Inorg. Chem.* **2006**, *45*, 1445–1462. (d) Yeh, R. M.; Raymond, K. N. *Inorg. Chem.* **2006**, *45*, 1130–1139. (e) Reid, S. D.; Blake, A. J.; Wilson, C.; Love, J. B. *Inorg. Chem.* **2006**, *45*, 636–643. (f) Hamacek, J.; Blanc, S.; Elhabiri, M.; Leize, E.; Van Dorsselaer, A.; Piguet, C.; Albrecht-Gary, A.-M. *J. Am. Chem. Soc.* **2003**, *125*, 1541–1550. (g) Fletcher, N. C.; Brown, R. T.; Doherty, A. P. *Inorg. Chem.* **2006**, *45*, 6132–6134. (h) Cucos, P.; Pascu, M.; Sessoli, R.; Avarvari, N.; Pointillart, F; Andruh, M. *Inorg. Chem.* **2006**, *45*, 7035–7037. (i) Argent, S. P.; Adams, H.; Riis-Johannessen, T.; Jeffery, J. C.; Harding, L. P.; Mamula, O.; Ward, M. D. *Inorg. Chem.* **2006**, *45*, 3905–3919. (j) Orita, A.; Nakano, T.; An, D. L.; Tanikawa, K.; Wakamatsu, K.; Otera, J. *J. Am. Chem. Soc.* **2004**, *126*, 10389–10396. (k) Saalfrank, R. W.; Spitzlei, C.; Scheurer, A.; Maid, H.; Heinemann, F. W.; Hampel, F. *Chem. Eur. J.* **2008**, *14*, 1472–1481. (l) Yeung, C. T.; Yeung, H. L.; Tsang, C. S.; Wong, W. Y.; Kwong, H. L. *Chem. Commun.* **2007**, 5203–5205. (m) Prabaharan, R.; Fletcher, N. C.; Nieuwenhuyzen, M. *J. Chem. Soc., Dalton Trans.* **2002**, 602–608.

10.1021/ic800856m CCC: $40.75 © 2008 American Chemical Society
Published on Web 10/11/2008

Scheme 1. Self-Assembly of Metal Ions with the Dis-N,O-bidentate Schiff Base Ligand Which Adopt Different Conformations

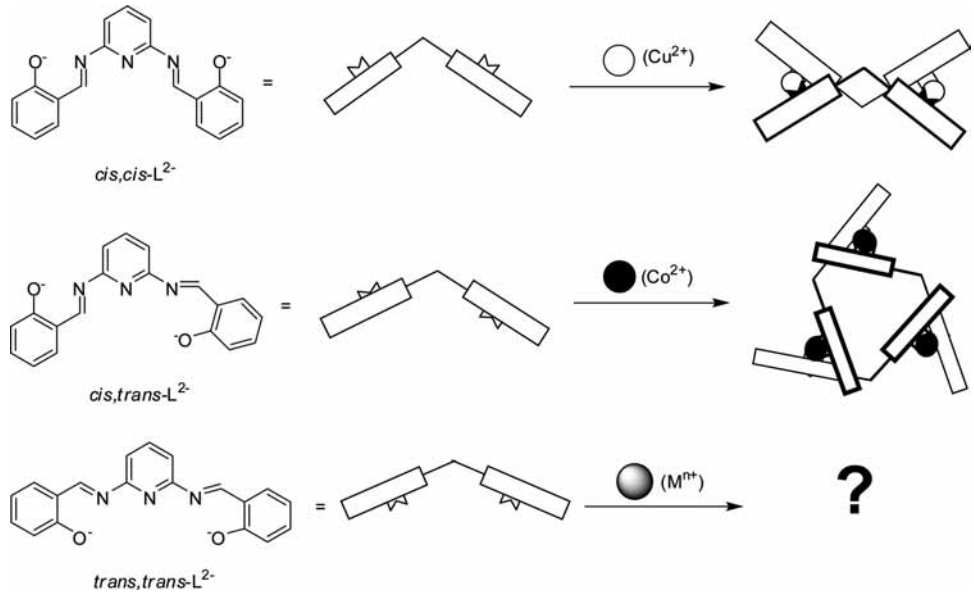

to prevent forming a mononuclear complex with only one metal ion. On the basis of these points of view, a series of symmetrical diimines containing pyridine as donor groups have been used to construct helicates.[6d,e,7] Besides, helicates based on (benz)imidazol, pyrrol, 2-quinoline, 2-hydroxybenzaldehyde, and so on have also been reported.[8−12] In the other reports, metal ions or solvent molecules can also determine whether the resulting complex will have a helical or mesostructure.[13,14]

Up to now, studies on helicates are focused on the understanding of fundamental principles of recognition and (self)-assembly processes. It is necessary to explore the potential application of helicates.[15,16] Our interests lie in not only the construction of helical structures from a self-assembly approach but also the development of magnetic materials with helical structures.[17] Therefore, we attempt to introduce 3d transition-metal ions as spin carriers into the fascinating helicate chemistry to prepare new functional molecular materials, such as chiral magnets[18] or helicates.[19] In this paper, we focus our attention on the new complexes linked by a Schiff base ligand, *N*,*N*′-bi(salicylidene)-2,6-pyridinediamine (H_2L, see Scheme 1).[20] The Schiff base is composed of three coplanar aromatic groups conjugated by the C═N bonds. When it reacted with Cu(II) salt, it was twisted to form a dinuclear mesocate. However, when it assembled with Co^{II} ions instead of Cu^{II} ions, a trinuclear Co^{II} complex with a pseudo C_3-symmetrical, torus-like molecular structure was formed, which can be regarded as a circular helicate. The structures and magnetic properties of both complexes have been investigated herein.

(6) (a) Ward, M. D. *Annu. Rep. Prog. Chem., Sect. A* **2002**, *98*, 285–320. (b) Cronin, L. *Annu. Rep. Prog. Chem., Sect. A* **2005**, *101*, 348–374. (c) Amabilino, D. B.; Stoddart, J. F. *Chem. Rev.* **1995**, *95*, 2725–2828. (d) Piguet, C.; Bernardinelli, G.; Hopfgartner, G. *Chem. Rev.* **1997**, *97*, 2005–2062. (e) Albrecht, M. *Chem. Rev.* **2001**, *101*, 3457–3497. (f) Piguet, C.; Borkovec, Hamacek, M.; Zeckert, J. K. *Coord. Chem. Rev.* **2005**, *249*, 705–726. (g) He, C.; Zhao, Y. G.; Guo, D.; Lin, Z. H.; Duan, C. Y. *Eur. J. Inorg. Chem.* **2007**, *345*, 1–3463. (h) Hou, J. Z.; Li, M.; Li, Z.; Zhan, S. Z.; Huang, X. C.; Li, D. *Angew. Chem., Int. Ed.* **2008**, *47*, 1711–1714. (i) Subramanian, P. S.; Suresh, E.; Casella, L. *Eur. J. Inorg. Chem.* **2007**, 1654–1660.

(7) See for examples: (a) Dong, G.; Pang, K. L.; Duan, C. Y.; Cheng, H.; Meng, Q. J. *Inorg. Chem.* **2002**, *41*, 5978–5985. (b) Lange, J.; Elias, H.; Paulus, H.; Muller, J.; Weser, U. *Inorg. Chem.* **2000**, *39*, 3342–3349. (c) Keegan, J.; Kruger, P. E.; Nieuwenhuyzen, M.; Martin, N. *Cryst. Growth Des.* **2002**, *2*, 329–332.

(8) (a) Yang, S. P.; Chen, X. M.; Ji, L. N. *J. Chem. Soc., Dalton Trans.* **2000**, 2337–2344. (b) Tuna, F.; Lees, M. R.; Clarckson, G. J.; Hannon, M. J. *Chem. Eur. J.* **2004**, *10*, 1472–1480.

(9) Yang, L.; Chen, Q.; Li, Y.; Xiong, S.; Li, G.; Ma, J. S. *Eur. J. Inorg. Chem.* **2004**, *147*, 8–1487.

(10) Hannon, M. L.; Paining, C. L.; Alcock, N. W. *Chem. Commun.* **1999**, 2023–2024.

(11) Yoshida, N.; Oshio, H.; Ito, T. *Chem. Commun.* **1998**, 63–64.

(12) (a) Mizumaki, S.; Houjou, H.; Nagawa, Y.; Kanesato, M. *Chem. Commun.* **2003**, 1148–1149. (b) Albrecht, M.; Janser, I.; Houjou, H.; Frölich, R. *Chem. Eur. J.* **2004**, *10*, 2839–2850. (c) Isola, M.; Liuzzo, V.; Marchetti, F.; Raffaelli, A. *Eur. J. Inorg. Chem.* **2002**, *158*, 8–1593.

(13) Pascu, M.; Clarkson, G. J.; Kariuki, B. M.; Hannon, M. J. *Dalton Trans.* **2006**, 2635–2642.

(14) (a) Xu, J.; Parac, T. N.; Raymond, K. N. *Angew. Chem., Int. Ed.* **1999**, *38*, 2878–2882. (b) Kreickmann, T.; Diedrich, C.; Pape, T.; Huynh, H. V.; Grimme, S.; Hahn, F. E. *J. Am. Chem. Soc.* **2006**, *128*, 11808–11819. (c) Simonneaux, G.; Kobeissi, M.; Toupet, L. *Inorg. Chem.* **2003**, *42*, 1644–1651. (d) Kam, K. C.; Young, K. L. M.; Cheetham, A. K. *Cryst. Growth Des.* **2007**, *7*, 1522–1532. (e) van Bebber, J.; Ahrens, H.; Fröhlich, R.; Hoppe, D. *Chem. Eur. J.* **1999**, *5*, 1905–1916. (f) Bruckner, C.; Brinas, R. P.; Bauer, J. A. K. *Inorg. Chem.* **2003**, *42*, 4495–4497. (g) Besli, S.; Coles, S. J.; Davies, D. B.; Eaton, R. J.; Hursthouse, M. B.; Kýlýc, A.; Shaw, R. A.; Yenilmez Ciftci, G.; Yesilot, S. *J. Am. Chem. Soc.* **2003**, *125*, 4943–4950. (h) Matsui, T.; Kim, S. H.; Jin, H.; Hoffman, B. M.; Ikeda-Saito, M. *J. Am. Chem. Soc.* **2006**, *128*, 1090–1091.

(15) Balzani, V.; Credi, A.; Raymo, F. M.; Stoddart, J. F. *Angew. Chem., Int. Ed.* **2000**, *39*, 3348–3391.

(16) Hotze, A. C. G.; Kariuki, B. M.; Hannon, M. J. *Angew. Chem., Int. Ed.* **2006**, *45*, 4839–4842.

(17) (a) Yamada, S.; Yasui, M.; Nogami, T.; Ishida, T. *Dalton Trans.* **2006**, 1622–1626. (b) Jensen, T. B.; Scopelliti, R.; Bünzli, J.-C. G. *Chem. Eur. J.* **2007**, *13*, 8404–8410. (c) Telfer, S. G.; Kuroda, R.; Lefebvre, J.; Leznoff, D. B. *Inorg. Chem.* **2006**, *45*, 4592–4601. (d) Sreerama, S. G.; Pal, S. *Inorg. Chem.* **2005**, *44*, 6299–6307. (e) Tangri, J.; Costa, J. S.; Aromí, G.; Mutikainen, I.; Turpeinen, U.; Gamez, P.; Reedijk, J. *Eur. J. Inorg. Chem.* **2007**, 4119–4122. (f) Tuna, F.; Lees, M. R.; Clarkson, G. J.; Hannon, M. J. *Chem. Eur. J.* **2004**, *10*, 5737–5750.

Table 1. Crystal Data and Structure Refinement Details for **1**·2CH_2Cl_2 and **2**·2CH_3OH·2CH_2Cl_2

	1·2CH_2Cl_2	**2**·2CH_3OH·2CH_2Cl_2
formula	$C_{40}H_{30}Cl_4Cu_2N_6O_4$	$C_{61}H_{51}Cl_4Co_3N_9O_8$
fw	927.58	1356.70
space group	*C*2/*c*	$P\bar{1}$
a (Å)	15.9894(13)	12.955(2)
b (Å)	14.3341(12)	14.489(3)
c (Å)	18.1981(15)	16.570(3)
α (deg)	90.00	88.823(3)
β (deg)	113.3310(10)	76.649(3)
γ (deg)	90.00	72.619(3)
V (Å^3)	3829.8(5)	2878.8(9)
Z	4	2
D_{calcd} (g cm^{-3})	1.609	1.565
F(000)	1880	1386
reflns collected/unique	10604/3796	9997/5809
GOF on F^2	1.036	0.999
R_1[a] [$I > 2\sigma(I)$]	0.0361	0.0929
wR_2[b]	0.0829	0.2270

[a] $R1 = \sum|F_o|$. [b] $wR2 = [\sum[w(F_o^2 - F_c^2)^2]/\sum[w(F_o^2)^2]]^{1/2}$.

Experimental Section

Materials. All chemicals were of reagent grade quality obtained from commercial sources and were used without further purification. The ligand H_2L was synthesized by condensation of 2,6-pyridinediamine with salicaldehyde in methanol following the literature method.[20]

General Characterization and Physical Measurements. The C, H, and N elemental analysis was conducted on a Perkin-Elmer 240C elemental analyzer with the samples dried in vacuum for 2 h. The FT-IR spectra were recorded from KBr pellets in the range of 4000−400 cm^{-1} on a Mattson Alpha-Centauri spectrometer. TGA was performed on a Perkin-Elmer TG-7 analyzer from 35 to 800 °C at a rate of 10.0 °C min^{-1} under nitrogen. Mass spectra were acquired using a Finnigan MAT LCQ mass spectrometer equipped with an electro-spray ionization (ESI) source. The spray voltage is 4.5 kV. The desolvation (nebulizing) gas temperature is 150 °C, and the sample solutions were pumped into the source at the flow rates of about 5 μL/min. The crystal sample of **2** used for MS analysis was prepared and treated with at vacuum or argon atmosphere. Temperature-dependent magnetic susceptibility data for polycrystalline complex of **1** and powder complex of **2** were obtained on a Quantum Design MPMS-XL SQUID magnetometer under an applied field of 1000 Oe over the temperature range of 2−300 K. The samples were packed into plastic films, which were then mounted in low-background diamagnetic plastic straws. The data were corrected for the diamagnetism of the constituent atoms using Pascal constants and the magnetization of the sample holder.

Preparation of Cu_2L_2 (1). H_2L (0.0317 g, 0.1 mmol) in CH_2Cl_2 (12 mL) was added to MeOH (4 mL) containing $Cu(OAc)_2$·2H_2O (0.0249 g, 0.1 mmol) with stirring and then heated to reflux for 0.5 h. The resulted solution was filtered after cooling to room temperature. The filtrate was allowed to stand at room temperature without disturbance. Dark green single crystals of **1**·2CH_2Cl_2 suitable for X-ray analysis were obtained after the solvent was evaporated slowly for one night, then collected by filtration, and dried in vacuum to afford solid 0.0394 g, yield: 52%. Elemental anal. Calcd for $C_{38}H_{26}Cu_2O_4N_6$ (%): C, 60.23; H, 3.46; N, 10.5. Found (%): C, 60.13; H, 3.51; N, 10.51. Selected IR bonds (KBr, cm^{-1}): 1611 (s), 1586(s), 1525 (s), 1430 (s), 1371 (m), 1326 (m), 1179 (s), 1143 (s), 1020 (w), 974 (w), 845 (w), 808 (w), 728 (m).

Preparation of Co_3L_3 (2). The complex of **2** was prepared according to the procedure of complex **1** except using $Co(OAc)_2$·4H_2O instead of $Cu(OAc)_2$·2H_2O in 15 mL of MeOH/CH_2Cl_2 (1:1, v:v). Red rhombic single crystals of **2**·2CH_3OH·2CH_2Cl_2 suitable for X-ray analysis were obtained by slow evaporation of the solvent for one night, yield: 89%. Elemental anal. Calcd for $C_{57}H_{39}Co_3O_6N_9$ (%): C, 60.98; H, 3.50; N, 11.23. Found (%): C, 60.63; H, 3.54; N, 11.41. Selected IR bonds (KBr, cm^{-1}): 1608 (s), 1578(s), 1521 (s), 1426 (s), 1374 (m), 1321 (m), 1172 (m), 1143 (s), 995 (w), 844 (s), 798 (m), 757 (m).

X-ray Crystallography. Single-crystal X-ray diffraction data for complexes **1**·2CH_2Cl_2 and **2**·2CH_3OH·2CH_2Cl_2 were performed on a Siemens SMART APEX CCD diffractometer with graphite-monochromated Mo Kα radiation (λ = 0.71073 Å) at 153 K.[21] Data were collected in the range of $1.99 < \theta < 26.04°$ for **1**·2CH_2Cl_2 and $1.70 < \theta < 25.03°$ for **2**·2CH_3OH·2CH_2Cl_2. Absorption corrections were applied using a multiscan technique. All the structures were solved by Direct Method of SHELXS-97 and refined by full-matrix least-squares techniques using the SHELXL-97 program.[22] Non-hydrogen atoms were refined with anisotropic temperature parameters. Hydrogen atoms were placed in calculated positions and refined using a riding model. Thermal ellipsoid plots of two structures are given in the Supporting Information. The detailed crystallographic data and structure refinement parameters for **1**·2CH_2Cl_2 and **2**·2CH_3OH·2CH_2Cl_2 are summarized in Table 1. CCDC reference numbers are 671836 for **1**·2CH_2Cl_2 and 671835 for **2**·2CH_3OH·2CH_2Cl_2.

Results and Discussion

Preparation of the Complexes. The ligand H_2L is composed of three aromatic groups conjugated by the C=N bonds. The aromatic groups provide a hydrophobic surface capable of participating in π-stacking or other van der Waals interactions. Each L^{2-} can be regarded as a dis(bidentate) donor set. The arrangement of two bidentate donor sets results in different conformations denoted as cis−cis, cis−trans, and trans−trans (Scheme 1), which may lead to different motifs of structure when coordinated with metal ions. When H_2L reacted with $Cu(OAc)_2$·2H_2O, a dinuclear mesocate would be obtained owing to the L^{2-} in cis−cis conformation; while when $Co(OAc)_2$·4H_2O was used in the

(18) (a) Sanmartìn, J.; Novio, F.; Garcia-Deibe, A. M.; Fondo, M.; Ocampo, N.; Bermejo, M. R. *Polyhedron* **2006**, *25*, 1714–1722. (b) Wen, H. R.; Wang, C. F.; Li, Y. Z.; Zuo, J. L.; Song, Y.; You, X. Z. *Inorg. Chem.* **2006**, *45*, 7032–7034. (c) Gu, Z. G.; Song, Y.; Zuo, J. L.; You, X. Z. *Inorg. Chem.* **2007**, *46*, 9522–9524. (d) Coronado, E.; Galán-Mascarós, J. R.; Gómez-García, C. J.; Murcia-Martínez, A. *Chem. Eur. J.* **2006**, *12*, 3484–3492. (e) Wang, X. Y.; Wei, H. Y.; Wang, Z. M.; Chen, Z. D.; Gao, S. *Inorg. Chem.* **2005**, *44*, 572–583. (f) Clemente-León, M.; Coronado, E.; Gómez-García, C. J.; Soriano-Portillo, A. *Inorg. Chem.* **2006**, *45*, 5653–5660. (g) Gao, E. Q.; Yue, Y. F.; Bai, S. Q.; He, Z.; Yan, C. H. *J. Am. Chem. Soc.* **2004**, *126*, 1419–1429.

(19) (a) Baum, G.; Constable, E. C.; Fenske, D.; Housecroft, C. E.; Kulke, T.; Neuburger, M.; Zehnder, M. *J. Chem. Soc., Dalton Trans.* **2000**, 945–959. (b) Bai, Y.; Duan, C. Y.; Cai, P.; Dang, D. B.; Meng, Q. J. *Dalton Trans.* **2005**, 2678–2680. (c) Sun, Q.; Bai, Y.; He, G.; Duan, C.; Lin, Z.; Meng, Q. *Chem. Commun.* **2006**, 2777–2779. (d) Mamula, O.; von Zelewsky, A.; Brodard, P.; Schläpfer, C.-W.; Bernardinelli, G.; Stoeckli-Evans, H. *Chem. Eur. J.* **2005**, *11*, 3049–3057. (e) Woods, C. R.; Benaglia, M.; Cozzi, F.; Siegel, J. S. *Angew. Chem., Int. Ed. Engl.* **1996**, *35*, 1830–1833. (f) Wang, Y.; Fu, H.; Shen, F.; Sheng, X.; Peng, A.; Gu, Z.; Ma, H.; Ma, J.; Yao, J. *Inorg. Chem.* **2007**, *46*, 3548–3556. (g) Sánchez-Quesada, J.; Seel, C.; Prados, P.; de Mendoza, J. *J. Am. Chem. Soc.* **1996**, *118*, 277–278. (h) Shinoda, S.; Okazaki, T.; Player, T. N.; Misaki, H.; Hori, K.; Tsukube, H. *J. Org. Chem.* **2005**, *70*, 1835–1843.

(20) Galić, N.; Matković-Ealogović, D.; Cimerman, Z. *J. Mol. Struct.* **1997**, *406*, 153–158.

(21) *Siemens, SMART*, Version. 5.05; Siemens Analytical X-ray Instruments Inc.: Madison, WI, 1995.

(22) Sheldrick, G. M. *SHELXS-97* and *SHELXL-97*, University of Göttingen: Göttingen, Germany, 1997.

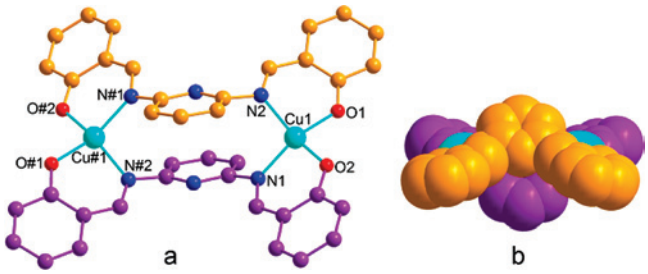

Figure 1. Left, ball-stick representation of **1** (blue green, Cu; red, O; blue, N; and purple, yellow colored C atoms from different ligands); right, space-filling model of **1,** ligand is shown in different color. H atoms are omitted for clarity.

Table 2. Selected Bond Lengths (Å) and Angles (deg) for **1**·$2CH_2Cl_2$ and **2**·$2CH_3OH$·$2CH_2Cl_2$

	1·CH_2Cl_2		
Cu1−O1	1.894(2)	Cu1−O2	1.902(2)
Cu1−N1	1.972(2)	Cu1−N2	1.970(2)
O1−Cu1−O2	89.5(7)	N1−Cu1−N2	97.3(8)
O1−Cu1−N2	151.1(8)	O2−Cu1−N2	93.5(8)
O1−Cu1−N1	93.1(8)	O2−Cu1−N1	152.3(8)
	2·$2CH_3OH$·$2CH_2Cl_2$		
Co1−O1	1.914(6)	Co1−O6	1.914(6)
Co1−N2	1.990(7)	Co−N9	2.003(7)
Co2−O2	1.911(6)	Co2−O3	1.921(5)
Co2−N5	1.988(7)	Co2−N3	1.998(7)
Co3−O4	1.886(6)	Co3−O5	1.941(6)
Co3−N8	2.007(7)	Co3−N6	2.020(7)
O1−Co1−O6	111.7(3)	O1−Co1−O6	111.7(3)
O1−Co1−N2	95.9(2)	O1−Co1−N2	95.9(2)
O6−Co1−N2	122.5(3)	O6−Co1−N2	122.5(3)
O2−Co2−O3	100.7(2)	O2−Co2−O3	100.7(2)
O2−Co2−N5	132.7(3)	O2−Co2−N5	132.7(3)
O3−Co2−N5	94.7(3)	O3−Co2−N5	94.7(3)
O4−Co3−O5	114.2(3)	O4−Co3−O5	114.2(3)
O4−Co3−N8	124.3(3)	O4−Co3−N8	124.3(3)
O5−Co3−N8	92.4(3)	O5−Co3−N8	92.4(3)

same preparing condition, a trinuclear helicate would be formed with the ligand L^{2-} in cis−trans conformation. Therefore, conformations of ligand and then the nuclearity and structures of the complexes are metal ion dependent. We also attempted to prepare complexes using other 3d ions such as Mn(II), Fe(III), Ni(II), and Zn(II) with this ligand. Unfortunately, no available single crystals were obtained. In addition, when other Cu^{II} (Co^{II}) salts (such as hydrochloricate, nitrate, or thiocyanate) were used, the target products would also be obtained in various yields.

Structure Description of 1·2CH₂Cl₂. The single-crystal X-ray analysis revealed that the reaction of H_2L with Cu^{II} gives rise to a double-strand dinuclear mesocate structure of Cu_2L_2, as shown in Figure 1. Selected bond distances and angles are listed in Table 2. Each of the Cu^{II} centers coordinates to the phenolic oxygen and imino nitrogen donors from two adjacent ligands. The average Cu−O and Cu−N distances are 1.898 and 1.971 Å, respectively, which are in the normal range. The coordination geometry of Cu^{II} centers is between square planar and tetrahedral (Figure 1), with the O(N)−Cu−N(O) angles being O1−Cu1−O2 (89.5°), N1−Cu1−N2 (97.3°), O1−Cu1−N1 (93.1°), O1−Cu1−N2 (151.1°), O2−Cu1−N1 (152.3°), and O2−Cu1−N2 (93.5°). Such an intermediate geometry has been previously observed with

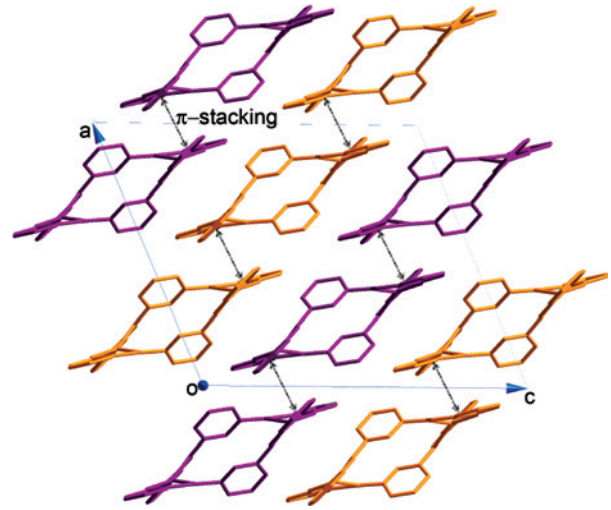

Figure 2. Representation of the F-type π-stacking interactions for **1**. Purple and yellow color the different chains formed by $\pi-\pi$ interaction. H atoms and solvent molecules are omitted for clarity.

other Cu^{II} ions, as caused by the geometric ligand strain,[23] as well as in a similar complex,[24c] which may be ascribed to the strong John-Teller effect of Cu^{II}. The ligands connect Cu^{II} centers in cis−cis conformation to form a mesocate. The pyridine rings from two coordinated ligands adopt an anti disposition, in which offset face-to-face π-stacking (F-type) interactions exist, with the slippage of 1.655 Å and centroid−centroid distance of 3.40 Å. The intracluster Cu···Cu distance separated by the pyridine spacer is 7.328 Å, which is slightly longer than other similar [Cu^{II}_2] complexes featuring the *m*-phenylene spacers.[24] Although dis(bidentate) salen-type Schiff-bases have been used to construct double strand dinuclear helicates,[6] it seems that the ligand in this complex is too rigid to form a helicate.

Each mesocate uses two phenyl rings from two donor sets of different ligands to connect the adjacent molecule by offset face-to-face π-stacking (F-type) interaction (Figure 2). The distance between the centroids of stacked phenyl rings is 3.629 Å. Thus, the molecules are connected one by one to form a compact and ordered chain along the diagonal direction of *a* and *c* axes. The distance between the two closest intercluster Cu^{II} centers (4.060 Å) is much shorter than the intracluster Cu−Cu distance (7.328 Å). Because of the distorted structure of the ligand, channels have been formed between the chains, and these channels are occupied by solvent molecules (Figure 3).

Structure Description of 2·2CH₃OH·2CH₂Cl₂. Single-crystal X-ray diffraction analysis showed that **2**·$2CH_3OH$·$2CH_2Cl_2$ crystallized in the triclinic $P\bar{1}$ space group. The complex possesses a pseudo threefold axis. It consists of an approximately equilateral triangle of cobalt(II) apexes with the ligands being the sides of the triangle. Each Co^{II} ion is

(23) Davis, W. M.; Zask, A.; Nakanishi, K.; Lippard, S. J. *Inorg. Chem.* **1985**, *24*, 3737–3743.
(24) (a) Hasty, E. F.; Wilson, L. J.; Hendrickson, D. N. *Inorg. Chem.* **1978**, *17*, 1834–1841. (b) Paital, A. R.; Mitra, T.; Ray, D.; Wong, W. T.; Ribas-Ariño, J.; Novoa, J. J.; Ribas, J.; Aromì, G. *Chem. Commun* **2005**, 5172–5174. (c) Paital, A. R.; Wu, A. Q.; Guo, G. C.; Aromì, G.; Ribas-Ariño, J.; Ray, D. *Inorg. Chem.* **2007**, *46*, 2947–2949.

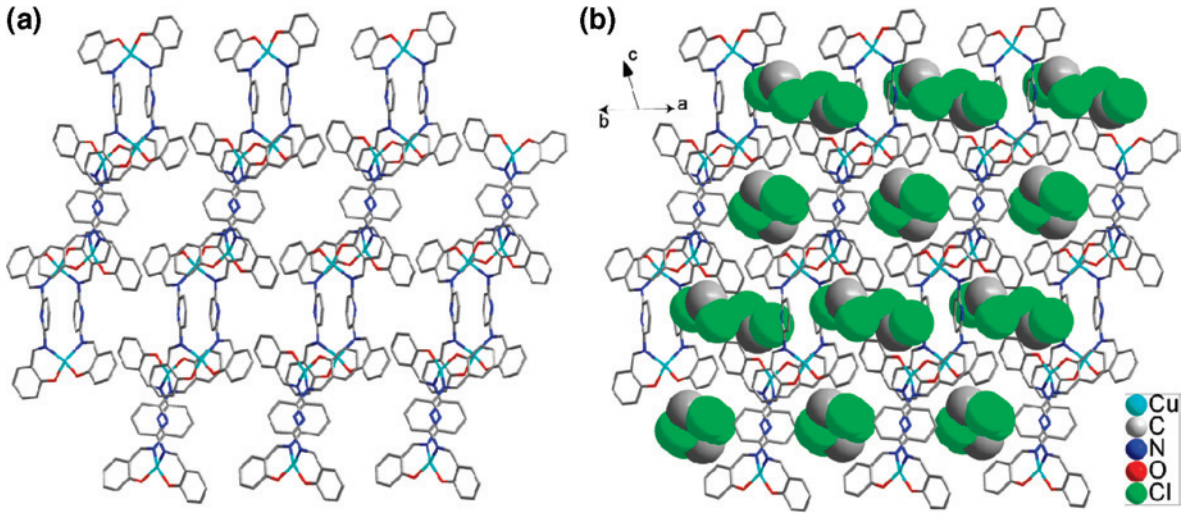

Figure 3. (a) Perspective view of the channels in packing structure of **1**·2CH_2Cl_2. (b) Solvent molecules are inside the intercluster channels. H atoms are omitted for clarity.

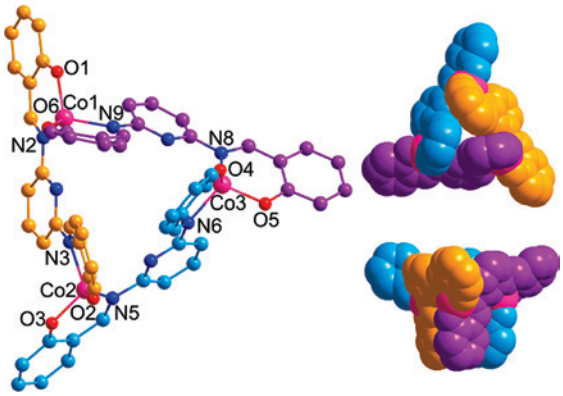

Figure 4. Left: ball-stick representation of **2** (pink, Co; red, O; blue, N; and light blue, purple, yellow colored C atoms from different ligands; only metal centers and coordinated atoms are labeled). Right: top view and side view of the molecular structure, to emphasize the helical nature each ligand is shown in a different color. H atoms are omitted for clarity.

coordinated by two dehydronated phenolic O atoms and two imine N atoms from two neighboring ligands to form a tetrahedral coordinated geometry (Figure 4). All of the Co−N and Co−O distances are in normal range (Table 2), with the average values of 2.001 Å for Co−N and 1.915 Å for Co−O, respectively. The N(O)−Co−O(N) angles range from 92.4(3) to 132.7(3)°, suggesting the coordination sphere around the Co ion to be distorted from the ideal tetrahedral arrangement. This underscores the fact that d^7 metals prefer this geometry if not constrained by other factors.[25] The different coordination spheres around Co and Cu is due to the weaker John-Teller effect in Co^{II} than that of Cu^{II}, corresponding to near tetrahedral and square planar coordination structure in the complex **1** and **2**, respectively; therefore, dinuclear and trinuclear complexes are obtained, respectively. The three ligands with twisted cis−trans conformation adopt a head-to-tail[6d] arrangement to encircle the triangular cobalt plane. A broad opening (formed by pyridine and cis-donor set) on one side of the plane and a narrow one (formed by trans-donor set) on the other side form a torus-like cluster structure in the solid state. When the arrangement of the aromatic rings around the broad opening is supposed as clockwise, the one on the narrow side will be counterclockwise. A CH_2Cl_2 molecule is on the top of torus (Figure S3, Supporting Information), which may contribute to the formation of such a circular, helical cluster with the broad opening and the narrow opening on each side. Moreover, each phenyl ring around the narrow opening contacts the neighboring intramolecular rings by T-type π-interaction, with an average H atom-to-centroid distance of 2.60 Å. Thus each circular and helical complex displays chirality. However, since both enantiomers are present in the lattice, the crystal is racemic.

The enantiomers are alternately disposed in the lattice. The aromatic rings around the broad openings connect the adjacent ones by both offset F-type and T-type interactions (Figure 5). The T-type π-interaction is between the phenyl rings around the broad openings and adjacent ones. These T-type stacks afford a pair of enantiomers that form a dimer and lead to the nearest intercluster Co···Co distance to be 4.899 Å between Co1 and Co3# (symmetry code: $1 - x$, $1 - y$, $-z$), which is even shorter than the intracluster distances. The dimers are connected one by one along the *b* axis to form a chain, and the chains further form a layer along the two diagonal directions of the *a* and *c* axes, both via F-type π-stacking. The centroid−centroid distances of these two kinds of F-type stacking are 3.766 Å and 3.841 Å, respectively. The spacing of the chains and the layers is occupied by solvent molecules (Figure 6).

The crystals of the complex **2** are brittle and easy to powder when exposed to air. It was suspected that Co^{II} might be oxidized to the Co^{III} state by aerial oxidation, since some similar examples had been reported before.[26] To confirm the stability of the complex **2**, ESI-MS was carried out on both the crystal and the powdered sample. The dominating *m*/*z* data are 318.8, 749.7, 1123.4, and 1496.8 for the crystal sample (Figure S4a, Supporting Information) and 749.5, 1123.2 and 1496.7 for the powdered sample (Figure S4b,

(25) Jaynes, B. S.; Doerrer, L. H.; Liu, S.; Lippard, S. J. *Inorg. Chem.* **1995**, *34*, 5735–5744.

(26) Banerjee, S.; Chen, J. T.; Lu, C. Z. *Polyhedron* **2007**, *26*, 686–694.

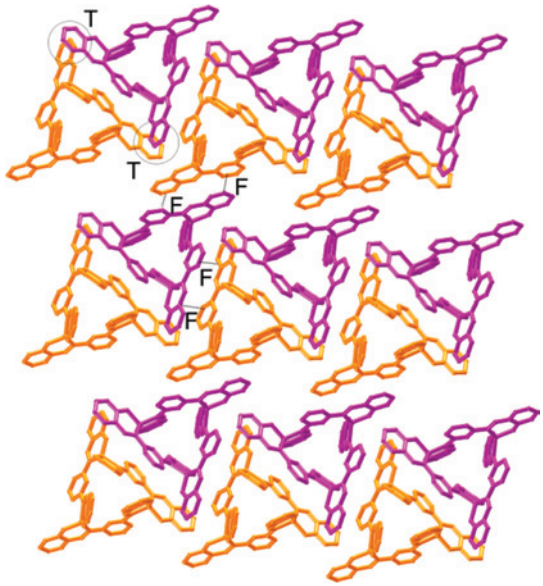

Figure 5. View of the layer formed by π-stacking interactions of $2\cdot 2CH_3OH\cdot 2CH_2Cl_2$. Different colors represent different chirality of the molecules (T represents the T-type and F represents the F-type π-stacking interactions). H atoms and solvent molecules were omitted for clarity.

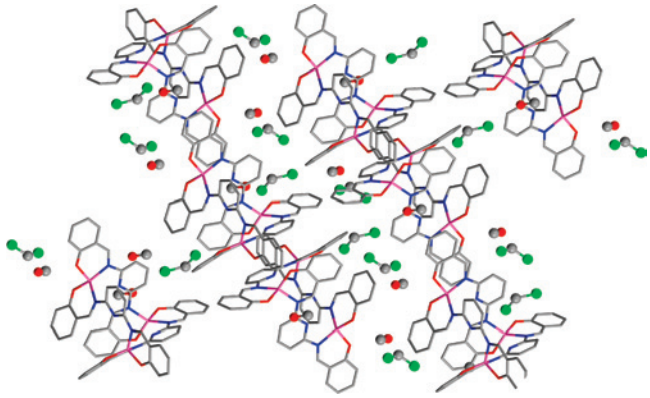

Figure 6. View of the packing structure of $2\cdot 2CH_3OH\cdot 2CH_2Cl_2$ along the *b* axes (pink, Co; red, O; blue, N; gray, C; green, chlorine). Solvent molecules are occupying the spacing of the chains and the layers. H atoms are omitted for clarity.

Supporting Information). The molecular ion peak at m/z = 1123 is consistent with the molecular weight of $[Co_3L_3]$. The molecular ion peaks at m/z = 749 and 1496 are ascribed to the fragment ion and the rearrangement ion, respectively. From the data above, it can be concluded that actually both the crystal and the powder have the same molecular weights. If the Co^{II} ions were oxidized to higher state, the molecular formula must be changed because of the charge balance, and thus the molecular weight would be different. Although ESI-MS measurements performed in solution were incapable of distinguishing between different solid state (the crystal and powder) structures, we can still confirm that Co^{II} did not oxidize to Co^{III} state when the crystal sample was exposed to air. The easy to powder for the crystal of complex **2** perhaps is due to the loss of solvent molecules.

Magnetic Properties. Temperature-dependent magnetic susceptibility data for polycrystalline complex of **1** and powder complex of **2** were measured at an applied magnetic field of 1000 Oe in the temperature range of 2−300 K. For

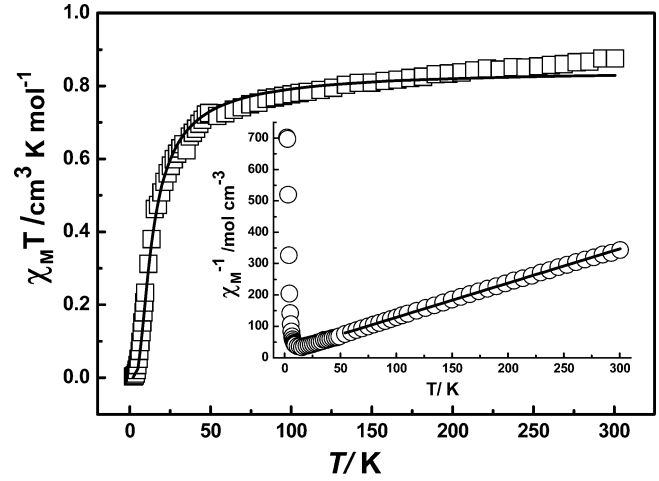

Figure 7. Plot of $\chi_M T$ versus T for **1**. Inset: Plot of χ_M^{-1} versus T. The solid black line is the theoretical fit of the data using the parameters given in the text.

1, the $\chi_M T$ value at 300 K is 0.83 cm^3 K mol^{-1}, which is slightly higher than the value expected for two uncoupled Cu^{II} centers (Figure 7). As temperature is lowered, $\chi_M T$ decreases smoothly to a value of 0.66 cm^3 K mol^{-1} at 37 K and then more abruptly below approximately 37 K, reaching a minimum value of 0.003 cm^3 K mol^{-1} at 2.0 K, which indicates the presence of antiferromagnetic coupling between Cu^{II} ions. It also can be found from the $\chi_M^{-1}-T$ plot (Figure 7, inset) that the thermal evolution of χ_M^{-1} above 50 K generally obeys Curie−Weiss law ($\theta = -17.9$ K and C_M = 0.92 cm^3 K mol^{-1}).

As early as 1978, Hendrickson and co-workers reported a very similar binuclear Cu^{II} complex, and it displayed weak antiferromagnetic property ($J = -1.0$ cm^{-1} in the Hamiltonian $H = -JS_1S_2$).[24a] Against this finding, in recent years, a series of structurally analogous dinuclear Cu^{II} complexes bridged by the substituted *m*-phenylene (*m*-N-Φ-N) ligands have been reported, which displayed ferromagnetic coupling between copper centers.[24b,c,27] The authors explained this phenomenon in terms of the spin-polarization mechanism. Herein, in complex **1**, again the antiferromagnetic interaction between Cu^{II} centers is found. To obtain insight into this experimental result, the data were fitted to the Bleaney−Bowers equation (eq 1).[28] The best fit of the data is represented by the solid line in Figure 7, which was calculated for $g = 2.13$, $J = -17.04$ cm^{-1}, and $R = 4.6 \times 10^{-4}$, where $R = \sum[(\chi T)_{obs} - (\chi T)_{calcd}]^2/\sum[(\chi T)_{obs}]^2$). Considering the intercluster interaction by the molecular-field approximation (eq 2), the fitted parameters for the complex of **1** are $g = 2.16$, $J = -15.29$ cm^{-1}, $zj' = -6.27$ cm^{-1}, and $R = 1.6 \times 10^{-4}$, confirming the antiferromagnetic interactions.

(27) (a) Fernández, I.; Ruiz, R.; Faus, J.; Julve, M.; Lloret, F.; Cano, J.; Ottenwaelder, X.; Journaux, Y.; Muñoz, M. C. *Angew. Chem., Int. Ed.* **2001**, *40*, 3039–3042. (b) Ottenwaelder, X.; Cano, J.; Journaux, Y.; Rivière, E.; Brennan, C.; Nierlich, M.; Ruiz-García, R. *Angew. Chem., Int. Ed.* **2004**, *43*, 850–850. (c) Glaser, T.; Heidemeier, M.; Grimme, S.; Bill, E. *Inorg. Chem.* **2004**, *43*, 5192–5194. (d) Pardo, E.; Faus, J.; Julve, M.; Lloret, F.; Munoz, M. C.; Cano, J.; Ottenwaelder, X.; Journaux, Y.; Carrasco, R.; Blay, G.; Fernandez, I.; Ruiz-Garcia, R. *J. Am. Chem. Soc.* **2003**, *125*, 10770–10771.
(28) Bleaney, B.; Bowers, K. D. *Proc. R. Soc. London, Ser. A* **1952**, *214*, 451–465.

$$\chi_M = \frac{2Ng^2\beta^2}{kT}\frac{1}{3+\exp(-J/kT)} \quad (1)$$

$$\chi = \frac{\chi_M}{1-(zj'/Ng^2\beta^2)\chi_M} \quad (2)$$

To further investigate the antiferromagnetism, DFT calculations were carried out on complex **1** using the UBPW91[29] function and the LANL2DZ[30] basis set. The structural parameters of complex **1** obtained from the crystallographic analysis were used for this calculation. The J value calculated through the broken-symmetry procedure ($J = [E(BS) - E(T)]$, where $E(T)$ is the energy for the triplet state and $E(BS)$ is the energy for the broken symmetry singlet) was found to be -35.6 cm^{-1}.

The selected atom Mulliken spin populations obtained from the calculations in the triplet state and the BS state for complex **1** are presented in Table S2 in the Supporting Information. In the BS state for **1**, the spin population on Cu1 is 0.4538, and those on the directly coordinated atoms (N1, N2, O1, and O2) have the same sign as that on Cu1. At the same time the spin populations on Cu1^i and on the directly coordinated atoms (N1^i, N2^i, O1^i, and O2^i) have the same sign and are opposite with the Cu1 group (Figure 8). This result demonstrates that the spin delocalization is from metal centers to the ligands in **1**. The spin population on C12 atom has different sign as that on N1 atom of the bridging ligand, and so does the C12^i with N1^i. It is obvious that Cu1−N1−C12−C8−N2^i−Cu1^i and Cu1−N2−C8^i−N3^i−C12^i−Cu1^i are antiferromagnetic pathways for **1**.

Compared with the N−Cu−N angles of the [Cu_2] system linked by the substituted *m*-phenylene (*m*-N-Φ-N) ligands (Table S1, Supporting Information), it can be concluded that the N−Cu−N angles may affect the magnetic coupling passing through the bridge between Cu^{II} centers. If the angle is close to 90° (smaller than 100°), the pathway would be antiferromagnetic; otherwise, if it is larger than 100°, the pathway would be ferromagnetic. Furthermore, the hetero N atom in the aromatic ring may also affect the magnetic coupling.

The temperature dependence of χ_M^{-1} and $\chi_M T$ of **2** was shown in Figure 9. The value of $\chi_M T$ at room temperature is smaller than three single Co^{II} ions in tetrahedral geometry (about 2.80 cm^3 K mol^{-1} of Co^{II} ion at 300 K). From 300 to

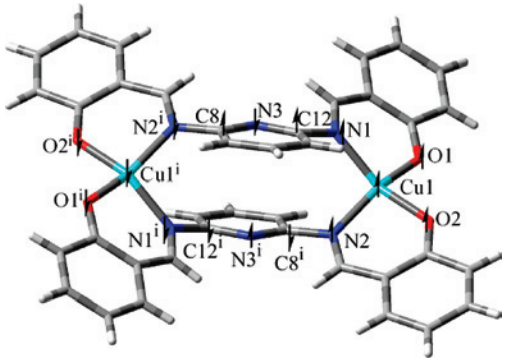

Figure 8. Signs of spin densities for complex **1** in the BS state. The arrow upward denotes positive spin density, and the arrow downward denotes the negative spin density.

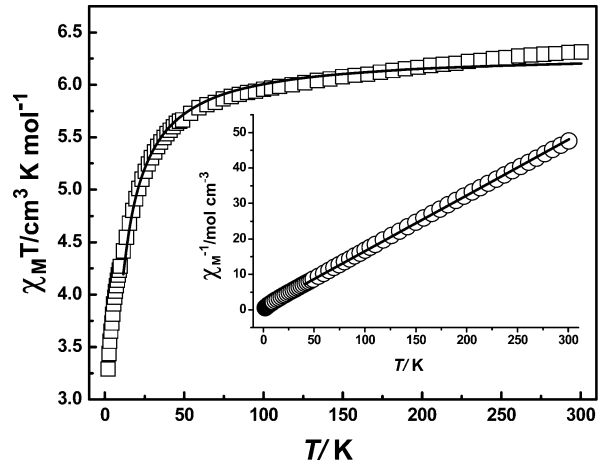

Figure 9. Plot of $\chi_M T$ versus T for **2**. Inset: Plot of χ_M^{-1} versus T. The solid black line is the theoretical fit of the data using the parameters given in the text.

54 K, the $\chi_M T$ values gradually decrease from 6.31 to 5.72 cm^3 K mol^{-1} and then more abruptly below approximately 41 K, reaching a minimum value of 3.28 cm^3 K mol^{-1} at 2.0 K, which indicates the antiferromagnetic coupling between Co^{II} ions. The thermal evolution of χ_M^{-1} above 40 K generally obeys Curie−Weiss law ($\theta = -5.34$ K and $C_M = 6.36$ cm^3 K mol^{-1}), which further indicates that the Co^{II} centers couple antiferromagnetically. Considering the Kramers degeneracy of Co(II) ions,[31b] the estimate of the g value and Weiss constant in the range 2−40 K are $g' = 4.53$ and $\theta' = -11.7$ K for the Co(II) centers with the effect spin state of 1/2. It should be noticed that triangular structure would lead to the spin frustration. In regularly triangular systems with half-integer spins, the ground-state can be represented as the orbital doublet ^{2}E.[31] Furthermore, in such systems the antisymmetric exchange (AS) term can lead to a specific zero-field splitting and magnetic anisotropy due to orbital contributions to the magnetic exchange. Thus, it is supposed that the zero-field splitting and orbital contributions afford higher experimental $\chi_M T$ values at low temperatures, with the effect spin state of 1/2 per Co^{II} ion.[31b] The examples of triangular Co_3 complexes are seldom found in the literature, and neither are models on this structure. In 2005, a theoretical treatment of a spin-frustrated trinuclear cobalt(II) system, in which the metal centers are also tetrahedrally coordinated, was developed by Berry and coworkers.[32] We used the following equation proposed by them to fit the experiment data of the complex **2** above 11.5 K:

(29) (a) Becke, A. D. *Phys. Rev. A* **1988**, *38*, 3098. (b) Perdew, J. P. In *Electronic Structure of Solids '91*; Ziesche, P., Eschig, H., Eds.; Akademie Verlag: Berlin, 1991; p 11.
(30) Dunning, T. H., Hay, P. J., Schaefer, H. F., III, Eds.; *Modern Theoretical Chemistry*; Plenum: New York, 1976; Vol. *3*, p 1.
(31) (a) Kahn, O. *Molecular Magnetism*; VCH Publishers: Berlin, 1993. (b) Carlin, R. L. *Magnetochemistry*; Springer Publishers: Berlin, 1986.
(32) Berry, J. F.; Cotton, F. A.; Liu, C. Y.; Lu, T. B.; Murillo, C. A.; Tsukerblat, B. S.; Villagrán, D.; Wang, X. P. *J. Am. Chem. Soc.* **2005**, *127*, 4895–4902.

$$\chi = (\chi_{||}(T) + 2\chi_{\perp}(T))/3$$

$$\chi_{||}(T) = \frac{N{g_{||}}^2\beta^2}{4kT} \times \frac{40e^{3j} + 105e^{8j} + 168e^{15j} + 165e^{24j} + 2\cosh(G/kT)}{8e^{3j} + 9e^{8j} + 8e^{15j} + 5e^{24j} + 2\cosh(G/kT)}$$

$$\chi_{\perp}(T) = \frac{N{g_{\perp}}^2\beta^2}{4kT} \times \frac{40e^{3j} + 105e^{8j} + 168e^{15j} + 165e^{24j} + (2kT/G)\sinh(G/kT)}{8e^{3j} + 9e^{8j} + 8e^{15j} + 5e^{24j} + 2\cosh(G/kT)}$$

Here, G represents the antisymmetric vector parameter and $g_{||}$, $g_{\perp}$, N, β, and k have their usual meaning.

The best-fit parameters for complex **2** are $J = -0.67$ cm^{-1}, $g_{||} = 2.37$, $g_{\perp} = 1.97$, $G = 0.0028$ cm^{-1}, and $R = 3.81 \times 10^{-3}$ (R is the agreement factor, defined as $\sum[(\chi_M T)_{obs} - (\chi_M T)_{calcd}]^2/\sum[(\chi_M T)_{obs}]^2$). Two reasons are responsible for the higher R value. One is that the intracluster Co···Co distances are longer and the interactions between Co^{II} centers will be weaker than the selected model. The other is that we did not consider the intercluster interactions. Therefore, it is necessary to develop a new specific model, and this work is in progress.

Conclusions

In this paper, we utilized a Schiff base ligand to prepare novel magnetic complexes with the aim to introduce 3d transition-metal ions as spin carriers into the fascinating helicate chemistry to afford new functional molecular materials, such as chiral magnets. Although the same synthetic condition was applied, the results are different: we obtained a mesocate of Cu_2L_2 with the ligand adopting a cis, cis conformation and a helicate of Co_3L_3 with the ligand adopting a cis, trans conformation. The structure of the mesocate is similar to the previously reported [Cu^{II}_2] systems with the *m*-phenylene diamine derivatived ligands. However, magnetic susceptibility data and DFT calculations revealed intracluster antiferromagnetic coupling for **1**. The complex of Co_3L_3 shows a torus-like molecular structure, which is the first X-ray characterized example of Co^{II}_3 circular helicate possessing antiferromagnetic interactions. Furthermore, the special structure of **2** affords a meaningful model to study the magnetic behavior based on triangular Co^{II} complex with spin frustration.

Acknowledgment. We thank the Natural Science Foundation of China (20274006; 20773022), NCET-06-0321, NENUSTB07007, and analysis and testing foundation of Northeast Normal University for financial support.

Supporting Information Available: Crystallographic data in CIF format, ORTEP diagrams, TGA analyses of complexes **1** and **2**, molecular magnetic orbitals of complex **1** in the high spin state, and other figures. This material is available free of charge via the Internet at http://pubs.acs.org.

IC800856M